

# THE FABRICATION OF THE $\beta = 0.12$ HWR AT RISP

G.T. Park\*, H. Kim, W.K. Kim, Y. Jung and H.J. Cha  
Rare Isotope Science Project (RISP), Daejeon, Korea

## Abstract

The fabrication of the  $\beta = 0.12$  half wave resonator (HWR) at RISP is complete. In this paper, we describe the fabrication process in detail: the material inspection, forming, machining, buffered chemical polishing (BCP) for the parts, the electron beam welding (EBW), and the clamp-up test followed by the final welding.

## INTRODUCTION

At RISP, a driver linac contains a SCL1-2 section consisting of the HWR's that accelerates the low-medium velocity ions. Earlier study on the beam dynamics determined the operation condition of the HWR as  $\beta = 0.12$ ,  $f = 162.5$  MHz with the accelerating voltage  $V_{acc} \sim 1.2$  MV.

In this paper, we report our progress on the fabrication of the HWR. The fabrication is complete now and the cavity is waiting to be processed and vertically tested. The vertical test can verify the performance of the cavity and also show some characteristic anomalies, i.e., the severe reduction of the  $Q_0$  value leading mostly to the quench at the lower gradient than targeted. The causes for the quenches most likely trace back to the imperfections during the fabrication process. For example, a poor welding in the strong current region of the cavity reduces the  $RRR$  value causing the early quench through the thermal instability. A failure to do vacuum furnacing is well known to cause the hydrogen Q-disease. These all trace back to the contamination of the RF surface. Thus it is utmost importance to maintain the defect-free RF surface within skin depth of about 50 nm. The important fabrication processes are summarized in Fig. 1.

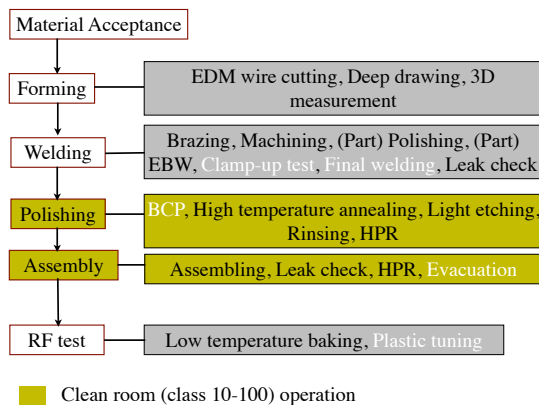


Figure 1: The fabrication process.

## MATERIAL INSPECTION

The 3 mm niobium sheet is purchased from Wah-Chang Inc. Its important material properties are summarized in Table 1. The high  $RRR$  is crucial to deter the quench by

Table 1: The Material Properties of the Niobium Obtained

Material properties	Value
$RRR$ value	>300
Grain size	<4 $\mu$ m
Recrystallization	100%

delivering the heat to the helium with the high thermal conductivity  $\lambda$ , which in turn comes from high  $RRR$  value, with the relation given as

$$\lambda(T = 4 \text{ K}) = \frac{RRR}{4}. \quad (1)$$

The grains must be small and uniform in size for a high formability. In addition, to spot the rust the de-ionized water dipping test is done for 24 hours (Fig. 2).

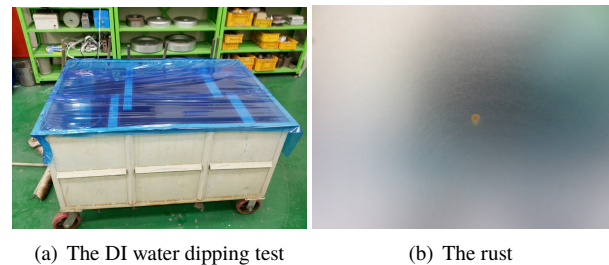


Figure 2: The DI water dipping test.

## FORMING

The niobium sheets were cut by the EDM wire cutting and deep drawn to form the parts. The niobium has very good formability and ductility with little spring back and does not work harden. The parts were pressed while controlling the pressure, velocity and hold time of the punch to avoid the tears or wrinkles (Fig. 3).

## NIOBIUM TO STAINLESS STEEL BRAZE TRANSITION

The helium vessel was designed to be stainless steel L316 (non-magnetized after the welding) with the thickness of 3 mm and encloses the 10 mm outside the bare cavity. Since the stainless thermally contracts more than the niobium in cool down, it could deform the cavity. So we introduced the bellows to the coupling ports at the upper and lower toroids

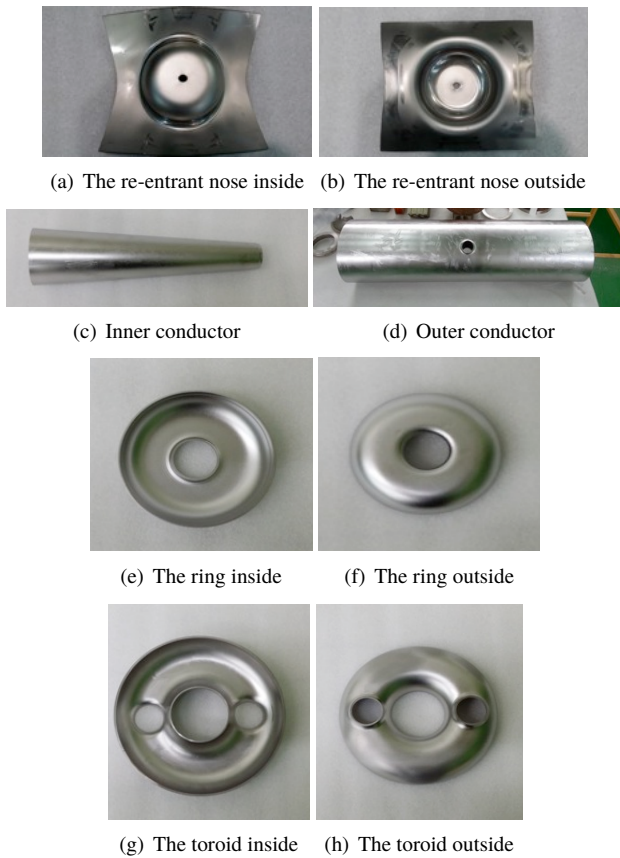


Figure 3: Formed parts of the HWR by deep drawing.

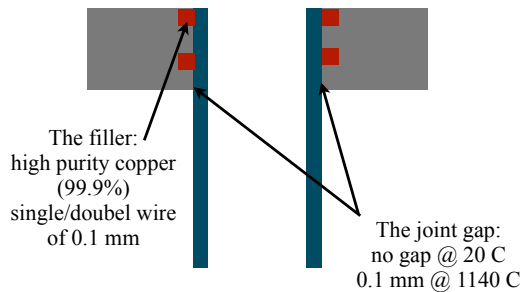


Figure 4: The joint design of the port.

where the contraction difference is large. The stainless flange and bellow are welded while the niobium port will be brazed to the flange. The joint design is shown in Fig. 4.

The filler metal dictated a brazing temperature. A typical furnace chart showing the brazing cycle is given in Fig. 5.

### ELECTRON BEAM WELDING (EBW)

The formed parts are electron beam welded in a high vacuum. The welding was done with the standard technique, i.e., to the full penetration with the defocused beam using the rhombic rasters.

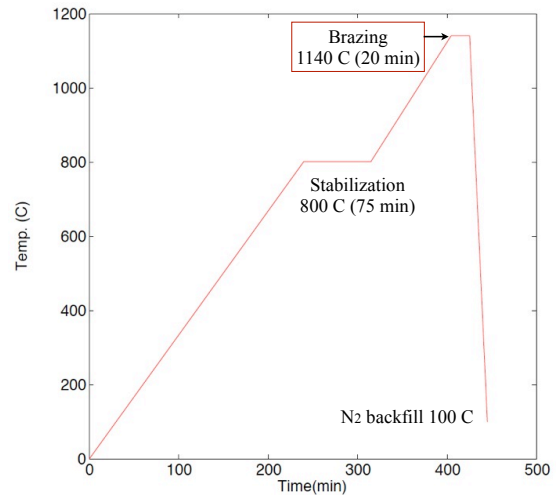


Figure 5: Thermal brazing cycle.

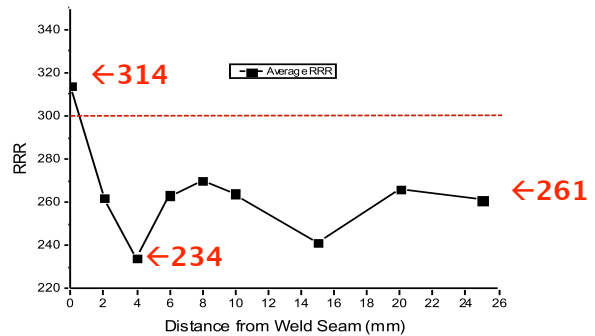


Figure 6: The RRR test of the Nb after the EBW (there is 9% reduction at lowest value and 5% reduction on average).

As a preparation of the EBW, the formed parts are machined while leaving the margin for the welding. Except for the re-entrant nose which is welded by butt-welding with 3 mm thickness, all the welding seams were machined to be 2 mm thick with the 0.5 mm step.

We performed the RRR test after the EBW of the niobium sample, whose result is shown in Fig. 6. The vacuum was set to be  $6 \times 10^{-5}$  torr. From Fig. 6, we see the maximum reduction of the RRR during the EBW takes place in the heat affected zone (HAZ), not near the welding seam. The reduction itself is rather severe, down to 235. The recovery to the pre-EBW value (RRR=314) as it goes out from the seam is not sufficient.

The welding conditions were carefully chosen after many trial-errors and listed in Table 2.

The optical inspection after the welding was performed to spot the bumps or the pits that could possibly cause the quench.

Table 2: The Welding Condition

Parameters	Value
Voltage	120 kV
Feeding speed	5 mm/sec
Focus size	0.5 mm
Distance	641 mm
Current	21 mA
Rastering frequency	4999 Hz
Vacuum	$6 \times 10^{-6}$ torr

### CLAMP UP TEST

The welded parts are clamped to measure the resonant frequency (see Fig. 7). The cavity had been prepared with the margin of about 10 mm at the (toroid) end of the inner and the outer conductors. To determine the target frequency after the final welding, we simulated a series of the coupled simulations to set up the target frequency table with a free boundary condition, see Table 3.

Table 3: The Target Frequency Table

Procedure	Frequency shift	Target frequency
Clamp-up	-	161.86 MHz
Final welding	270 kHz	162.13 MHz
Polishing	72.6 kHz	162.21 MHz
Evacuation	-4 kHz	162.21 MHz
Cool down	345 kHz	162.55 MHz
Tuner commission	-50 kHz	162.5 MHz

We assumed that the welding contraction is by 0.6 mm, the BCP will be done by 150  $\mu$ m, and the cool down is from 293 K to 2 K.

We trimmed the inner and outer conductors a few times to obtain the corresponding frequency shift. The measured data is shown in Table 4 and Fig. 8.

Table 4: The Clamp up Test Data

$l$ (mm)	$f$ (MHz)	$\Delta f$ (kHz)	$\Delta f/\Delta l$ (kHz/mm)
0	158.95	-	-
4.1	159.87	920	224
7.15	161.22	1350	443
8.2	161.51	290	276
9.3	161.85	340	309

Here  $l$  is the trimmed length. The average frequency shift is estimated as 312 kHz/mm.

Based on the clamp-up data up to 8.2 mm trimming, we estimated the length of the final cut to be 1.1 mm assuming the welding contraction to be 0.9 mm. The frequency measured met the expectation. But the frequency after the final welding is 161.94 MHz. The measured trimmed length was about 0.7 mm implying the frequency shift is only 129 kHz. This error is apparently introduced by the lack of dimensional corrections over many hours before the final welding.

ISBN 978-3-95450-142-7



Figure 7: Clamp up of the HWR.

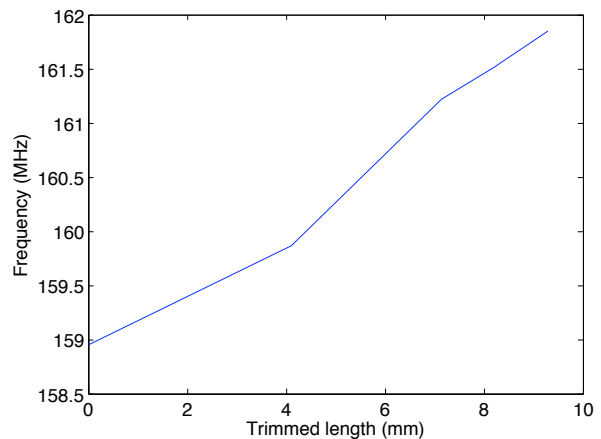


Figure 8: The frequency shift in clamp-up test.

### ACKNOWLEDGMENT

Special thanks go to Hyung Jin Kim and Dong-O Jeon, who guided us to learn and conduct the research on this project. This work was supported by the Rare Isotope Science Project which is funded by the Ministry of Science, ICT and Future Planning (MSIP) and the National Research Foundation (NRF) of the Republic of Korea under Contract 2011-0032011.